

CHROM. 9026

## DETERMINATION OF THE PRE-EXPONENTIAL FACTOR OF HENRY'S CONSTANT BY GAS ADSORPTION CHROMATOGRAPHY

J. GAWDZIK, Z. SUPRYNOWICZ and M. JARONIEC

*Department of Physical Chemistry, Institute of Chemistry UMCS, 20031 Lublin, Nowotki 12 (Poland)*

(Received December 12th, 1975)

---

### SUMMARY

The pre-exponential factor of Henry's constant is important in studies of heterogeneity effects and is required for evaluating the correct distribution of adsorption energy. This factor has been determined by gas adsorption chromatography using experimental retention volumes measured for different adsorbate pressures and temperatures. The retention data of benzene, *n*-hexane and cyclohexane on porous glass beads were studied in detail.

---

### INTRODUCTION

The problem of finding the energy distribution of heterogeneous adsorbents has been considered in great detail in recent years<sup>1-3</sup>, and the application of gas adsorption chromatography has also been considered<sup>4-10</sup>. In almost all of the chromatographic methods proposed for evaluating the distribution function of adsorption energy, a relation  $p = f(\epsilon)$  between the adsorbate pressure ( $p$ ) and adsorption energy ( $\epsilon$ ) was used<sup>4-6,8-10</sup>. The function  $f(\epsilon)$  depends on the choice of an equation for the local adsorption<sup>8,11,12</sup> (this equation describes the behaviour of the adsorbate on a homogeneous patch of the adsorbent surface).

Let us consider the inverse relation to  $p = f(\epsilon)$ , i.e.,  $\epsilon = \tilde{f}(p)$ . It follows from the literature<sup>8,12</sup> that the adsorption energy ( $\epsilon$ ) in the condensation approximation method can be expressed by

$$\epsilon = \epsilon^L + \epsilon_0 \quad (1)$$

where

$$\epsilon^L = RT \ln \frac{K}{p} \quad (2)$$

is the relation  $\epsilon = f(p)$  for local Langmuir behaviour,  $\epsilon_0$  is a characteristic energy depending on the local adsorption model, and  $K$  is the pre-exponential factor of Henry's constant (this factor is different for the mobile and localized adsorption models<sup>11,13</sup>). The characteristic energies ( $\epsilon_0$ ) were discussed in our previous papers<sup>8,12</sup>.

In this paper, we consider the problem of the numerical calculation of  $K$  from

chromatographic data. This constant mainly affects the position of the energy distribution function,  $\chi(\varepsilon)$ , on the energy axis<sup>3,11,14,15</sup> and slightly changes the form of  $\chi(\varepsilon)$ <sup>14,15</sup>. Using the condensation approximation method, we can observe only the influence of  $K$  on the position of  $\chi(\varepsilon)$  on energy axis<sup>5</sup>. The known chromatographic methods for evaluating the  $\chi(\varepsilon)$  are based on the condensation approximation and therefore in these methods only the shift effect of  $\chi(\varepsilon)$  can be observed.

It follows from the above discussion that  $K$  is important in studies of heterogeneity effects, and is particularly important in the evaluation of the distribution functions for adsorption systems that have different adsorbates, because it regulates the mutual positions of the functions  $\chi(\varepsilon)$ .

The available theoretical equations for calculating  $K$  require a knowledge of the molecular partition functions for molecules in the bulk and adsorbed phases<sup>11,13,16,17</sup>. Theoretical calculations of the partition functions are often complicated for organic vapours<sup>18-20</sup>, whereas organic substances are very often used in gas adsorption chromatography. The simpler methods<sup>3,12,13,21</sup> for the determination of  $K$  can be used either for simple gases or at low temperatures. However, the temperatures used in gas chromatography are usually in the range 300-400 °K. Therefore, the most substantiated method for calculating  $K$  seems to be that based on the measurement of retention data at different temperatures.

## THEORETICAL

We shall now consider the problem of determining  $K$  from experimental retention data. In our previous papers<sup>9,10</sup>, we proposed the following expression for describing the retention volume on heterogeneous adsorbents:

$$V_{N,t}(p) = \exp \left( \sum_{i=0}^m B_i p^i \right) \quad (3)$$

where  $p$  is the adsorbate pressure, the coefficients  $B_i$  are suitable parameters and the subscript  $t$  denotes the retention volume for a heterogeneous surface. Eqn. 3 is valid for the adsorbate phase treated as an ideal phase. However, for a non-ideal adsorbate phase, eqn. 3 can be expressed by

$$V_{N,t}(\rho) = \exp \left( \sum_{i=0}^m B'_i \rho^i \right) \quad (4)$$

where  $\rho$  is the adsorbate density in the free gas phase and the coefficients  $B'_i$  are related to the coefficients  $B_i$  by the equation

$$B'_i = (RT)^i B_i \quad (5)$$

Eqn. 4 can be treated as an exponential virial expansion for retention volume  $V_{N,t}$ . The equation analogous to eqn. 4 was used for adsorption isotherms by Rudziński<sup>22</sup>. It follows from the numerical calculations that the expansions 4 and 3 are more effective than the usual expansion<sup>23,24</sup>

$$V_{N,t}(\rho) = \sum_{i=0}^m \beta_i \rho^i \quad (6)$$

where  $\beta_i$  are the expansion coefficients.

Let us analyze eqn. 3 in detail. In a previous paper<sup>9</sup>, we showed that eqn. 3 is connected with the Jovanović adsorption model<sup>25-28</sup>. Assuming this model is valid for the retention mechanism, we obtain the following equation:

$$V_{N,t}(p) = \exp(B_0 + B_1 p) \quad (7)$$

where

$$\exp(B_0) = \frac{FRT N_m}{K} \cdot \exp\left(\frac{\varepsilon}{RT}\right) \quad (8)$$

and

$$B_1 = -\frac{1}{K} \cdot \exp\left(\frac{\varepsilon}{RT}\right) \quad (9)$$

$F$  is the James-Martin compressibility factor,  $N_m$  is the capacity of the adsorbed phase (monolayer capacity) and  $K$  and  $\varepsilon$  are as defined earlier. The subscript  $l$  denotes a homogeneous adsorbent surface.

Let us consider the patchwise heterogeneous surface of the adsorbent. The retention volume  $V_{N,t}$  can be expressed by

$$V_{N,t}(p) = \sum_{j=1}^n V_{N,t}^{(j)}(p, \varepsilon_j) \quad (10)$$

where  $V_{N,t}^{(j)}$  describes the retention volume for  $j$ th homogeneous patch of the adsorbent surface. Expressing  $V_{N,t}^{(j)}$  in eqn. 10 by eqn. 7 for  $p = 0$  (the case of linear chromatography):

$$V_{N,t}^{(j)} = \frac{FRT N_{mj}}{K_j} \cdot \exp\left(\frac{\varepsilon_j}{RT}\right) \quad (11)$$

we obtain

$$\exp(B_0) = V_{N,t}(p) = FRT \sum_{j=1}^n \frac{N_{mj}}{K_j} \cdot \exp\left(\frac{\varepsilon_j}{RT}\right) \quad (12)$$

where  $n$  is the number of the homogeneous patches,  $N_{mj}$  is the capacity of the  $j$ th homogeneous patch and  $K_j$  and  $\varepsilon_j$  denote the constant  $K$  and adsorption energy  $\varepsilon$ , respectively, for the  $j$ th patch. The studies of Hoory and Prausnitz<sup>29</sup> showed that the constants  $K_j$  are very similar for different patches. Thus, the adsorption system can be characterized by one constant,  $K$ , which is the average of all values of  $K_j$ . Therefore, eqn. 12 can be written in the form

$$\exp(B_0) = \frac{FRT N_m}{K} \cdot \sum_{j=1}^n \delta_j \cdot \exp\left(\frac{\varepsilon_j}{RT}\right) \quad (13)$$

where

$$\delta_j = N_{mj}/N_m \quad 0 < \delta_j \leq 1 \quad (14)$$

Finally, eqn. 13 can be written as

$$\exp(B_0) = \frac{FRT N_m}{K} \cdot \exp\left(\frac{\varepsilon}{RT}\right) \approx \frac{FRT N_m}{K} \cdot \exp\left(\frac{\bar{\varepsilon}}{RT}\right) \quad (15)$$

where  $\bar{\varepsilon}$  should be treated as an "exponential" average adsorption energy.

The constant  $K$  is temperature dependent<sup>3,16,17</sup>. At high temperatures,  $K$  for monoatomic gases is proportional to  $(T^{-0.5})^{13,16,30}$ :

$$K_{loc} = c_{loc} T^{-0.5} \quad (16)$$

for the localized adsorption model, and to  $T^{0.5}$

$$K_{mob} = c_{mob} T^{0.5} \quad (17)$$

for the mobile adsorption model. The subscripts loc and mob denote the localized and mobile adsorption models;  $c_{loc}$  and  $c_{mob}$  are the proportionality coefficients.

Numerical calculations indicate that temperature dependence of the constants  $K_{loc}$  and  $K_{mob}$  for other adsorbates at high temperatures is small. The real adsorption systems should obey an indirect model. Therefore, with good approximation the temperature dependence of  $K$  at high temperatures can be neglected. Let  $\bar{K}$  denote the temperature-independent constant  $K$ . Then, eqn. 15 can be written in the following linear form:

$$B_0 - \ln T = \ln \left( \frac{FR N_m}{\bar{K}} \right) + \frac{\bar{\varepsilon}}{RT} = a + \frac{b}{T} \quad (18)$$

where

$$a = \ln \left( \frac{FR N_m}{\bar{K}} \right); b = \frac{\bar{\varepsilon}}{R} \quad (19)$$

Eqn. 18 shows that the plot of  $B_0 - \ln T$  against  $1/T$  should yield a straight line of slope  $\bar{\varepsilon}/R$  and intercept  $a$ . The calculation of  $\bar{K}$  is possible if  $N_m$  is known. Monolayer capacity  $N_m$  values can be calculated from the equation

$$\bar{N}_m = \frac{-1}{k} \sum_{i=1}^k [FRT_i B_1(T_i)]^{-1} \cdot \exp [B_0(T_i)] \quad (20)$$

where  $\bar{N}_m$  is the average of all  $N_m$  values obtained for different temperatures and  $k$  is the number of experimental functions  $V_{N,i}(p)$  measured for different temperatures. Eqn. 20 can be derived from an earlier equation for calculating the specific surface area<sup>31</sup> or from eqns. 8 and 9.

Eqns. 16 and 17 can be represented by one equation:

$$K = c T^r \quad (21)$$

where  $c$  is the temperature-independent constant; however,  $r \in (-0.5, 0.5)$  and  $r$  can be treated as a best-fit parameter. From eqns. 15 and 21, we obtain the following linear form:

$$B_0 - \ln T^{1-r} = \ln \left( \frac{FR N_m}{c} \right) + \frac{\bar{\varepsilon}}{RT} \quad (22)$$

Using eqn. 22, we can take into account the temperature dependence of  $K$  at high temperatures.

## EXPERIMENTAL

*Preparation of the adsorbent*

Controlled-pore glass beads<sup>32</sup> were used as an adsorbent in chromatographic measurements, and were prepared in this Department from sodium borosilicate glass, the molar percentage composition of which was 7% Na<sub>2</sub>O, 23% B<sub>2</sub>O<sub>3</sub> and 70% SiO<sub>2</sub>. In the glassworks, the glass was melted, poured into cold water, crushed in a steel mortar, milled in a ball-mill and fractionated by screening. The 0.15–0.20-mm fraction was used to prepare the glass beads (ideally spherical) in a special gas burner. The beads were again screened and the 0.15–0.20-mm fraction was leached in 2 *N* sodium hydroxide solution at 95 °C for 0.5 h in order to remove the thin layer of glass on the surface of the beads, which has a different composition from the glass inside<sup>33</sup>. The beads were then washed with distilled water until neutral and dried at 120 °C for 24 h in a laboratory oven. The dry beads were heat-treated in a porcelain crucible in an electrical muffle furnace at 600 ± 1 °C for 6 h<sup>34</sup>. The temperature was controlled by using a chromel–alumel thermocouple. At the end of the treatment, the crucible was removed from the furnace and the beads were air cooled. The time of heat treatment was measured from the moment the crucible reached the oven temperature (about 15 min after placing the crucible in the oven).

The heat-treated beads were leached by stirring with 5 *N* sulphuric acid at 95 °C for 10 h according to Hood and Nordberg<sup>33</sup>. The proportions of the glass beads to the acid were 100 g to 1.5 l. The acid was then decanted off and the beads were washed repeatedly with water until the supernatant liquid was neutral and free from visible colloidal silica. In order to remove the colloidal silica that was precipitated in the large pores, a 2-h treatment with 0.5 *N* sodium hydroxide solution at 25 °C was applied according to the procedure described by Zdanov<sup>35</sup> and Wolf<sup>36</sup>. The beads were then washed with water until neutral, stirred with cold 3 *N* hydrochloric acid for 2 h and again washed with water until neutral. Next they were dried in a laboratory oven at 120 °C for 24 h. In order to remove the remainder of the micropores<sup>37,38</sup>, the beads were treated in a muffle furnace at 700 ± 1 °C for 2 h, then stirred with 5 *N* hydrochloric acid at 95 °C for 10 h to obtain a clean and fully hydroxylated surface<sup>39</sup>. Finally, the beads were washed with distilled water until neutral and dried at 120 °C for 24 h. During each digestion process, the proportions of 1.5 l of digesting solution to 100 g of the beads was maintained.

*Measurement of surface area, pore volume and pore size distribution*

Nitrogen adsorption measurements were performed at 78 °K on controlled-pore glass beads by two different methods: the Nelsen–Eggertsen thermal desorption method (home-made apparatus) and the volumetric method with a Sorptomatic 1806 instrument (Carlo Erba, Milan, Italy). The surface area was calculated by the B.E.T. method using 16.2 Å<sup>2</sup> as the area of coverage per nitrogen molecule. The results of the surface area measurements are given in Table I. The adsorption and desorption isotherms and pore size distribution curve calculated from the Sorptomatic data according to Barrett *et al.*<sup>40</sup> and Wheeler<sup>41</sup> are presented in Fig. 1 and Table I.

The porosimetric analysis was performed on a Model 1520 mercury porosimeter (Carlo Erba). The results are given in Fig. 2 and Table I.

TABLE I  
PARAMETERS CHARACTERIZING THE POROUS GLASS BEADS INVESTIGATED

| Specific surface area, $S$ ( $\text{m}^2/\text{g}$ ) | Pore radius at maximum pore size distribution, $R_{\text{max}}$ ( $\text{\AA}$ ) | Total volume of pores, $v$ ( $\text{ml}/\text{g}$ ) |
|--|--|---|
| 69.5*  | 145*   | 0.77*   |
| 71.5**   | 130***   | 0.64***   |

\* Calculated from Sorptomatic data.

\*\* Calculated by using Nelsen-Eggertsen method.

\*\*\* Calculated from porosimetric data.

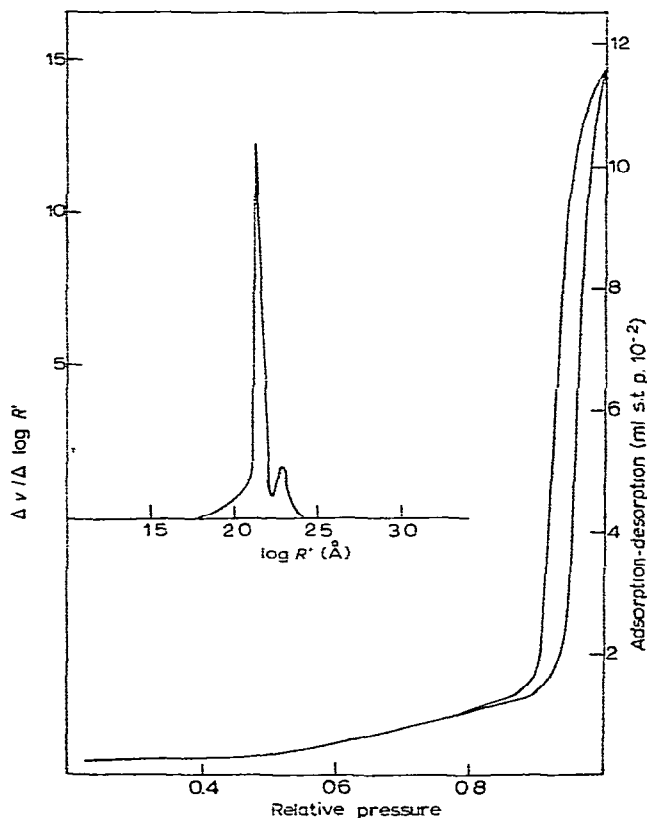


Fig. 1. Adsorption and desorption isotherms of nitrogen on the porous glass beads at the temperature of liquid nitrogen and differential pore size distribution,  $\Delta v/\Delta \log R'$ , as a function of  $\log R'$ . Experimental data from Sorptomatic.

#### Chromatographic measurements

The measurements were carried out on a Chromatron GCHF 18.3 gas chromatograph (G.D.R.) with a thermal conductivity detector. Hydrogen purified by using a filter containing molecular sieve 5A pellets was used as the carrier gas at a flow-rate

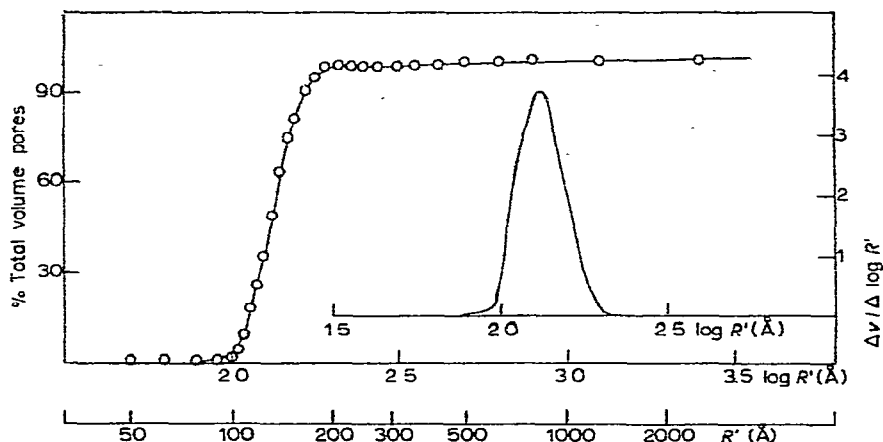


Fig. 2. Integral and differential pore size distribution,  $\Delta v/\Delta \log R'$ , for the porous glass beads obtained with the Porosimeter.

of 50 cm<sup>3</sup>/min. The glass chromatographic column (92 cm × 4 mm I.D.) contained 6.28 g of adsorbent. Before measurements, the column packing was conditioned with carrier gas at 473 °K for 12 h. The measurements were performed at 328, 343, 358 and 373 °K; The stability of the column temperature was  $\pm 0.1$  °K. The temperature of the injector was 473 °K. Benzene and cyclohexane (pro analysi grade) from Polskie Odczynniki Chemiczne (Gliwice, Poland) and *n*-hexane (99% pure) from Reachim (Moscow, U.S.S.R.) were used as adsorbates. The calibration of the detector on the GLC column was performed by injecting 1-, 10- and 50- $\mu$ l volumes with Hamilton microsyringes into the column containing the partition packing (10% E-30 on 100–120-mesh siliconized Diatomite C; Pye Unicam, Cambridge, Great Britain)<sup>42</sup>.

The experimental  $V_{N,t}$  versus  $p$  data were obtained by using the peak maxima elution method<sup>43</sup>, and the results are shown in Figs. 3–5, which also show the adsorption isotherms corresponding to the functions  $V_{N,t}(p)$ . The adsorption isotherms were calculated according to the method described in our previous paper<sup>9</sup>.

## RESULTS AND DISCUSSION

The experimental functions  $V_N(p)$  in Figs. 3–5 were approximated by using the following polynomial approximation (see eqn. 3):

$$\ln V_{N,t}(p) = \sum_{i=0}^m B_i p^i \quad (23)$$

As a criterion of the best approximation, we used the sum of the squared deviations, which is defined by

$$S_m = \sum_{i=1}^L \left[ \ln V_{N,t}(p_i) - \sum_{i=0}^m B_i (p_i)^i \right]^2 \quad (24)$$

where  $L$  is the number of experimental points.

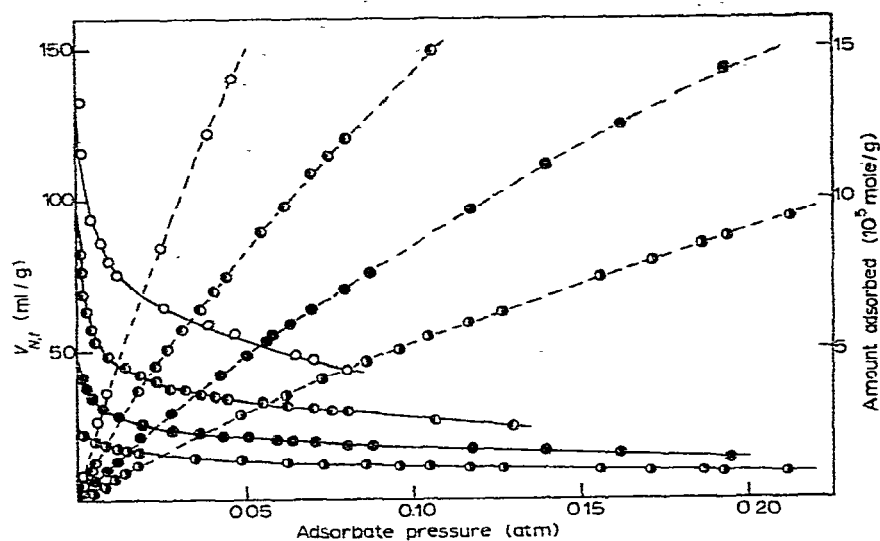


Fig. 3. Adsorption of benzene on the porous glass beads. The solid lines denote approximations for the experimental functions  $V_{N,t}(p)$ . The dashed lines denote the adsorption isotherms calculated by using the approximations in eqn. 3. Circles denote the experimental points of retention volume or adsorption: ○, 328°K; ◐, 343°K; ●, 358°K; ⊖, 373°K.

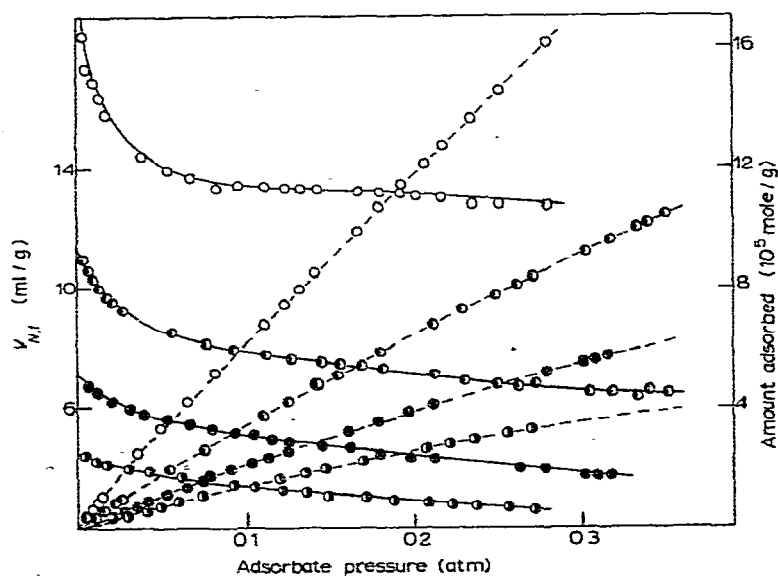


Fig. 4. Adsorption of *n*-hexane on the porous glass beads. The solid lines denote the functions  $V_{N,t}(p)$ , and the dashed lines denote the adsorption isotherms for different temperatures: ○, 328°K; ◐, 343°K; ●, 358°K; ⊖, 373°K.



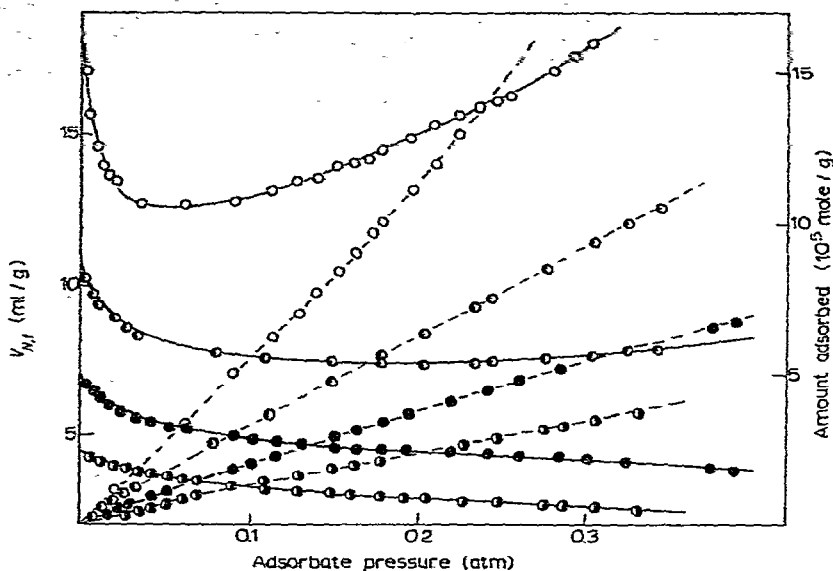


Fig. 5. Adsorption of cyclohexane on the porous glass beads. The solid lines denote the functions  $V_{N,1}(p)$ , and the dashed lines denote the adsorption isotherms for different temperatures:  $\circ$ , 328°K;  $\bullet$ , 343°K;  $\bullet$ , 358°K;  $\bullet$ , 373°K.

The degrees ( $m$ ) of the best polynomials and sums of the squared deviations are summarized in Table II, which also gives the numerical values of  $\exp(B_0)$ ,  $B_1RT \exp(B_0)$  and  $\exp(B_0)/(RTFB_1)$ . Using the numerical values of  $\exp(B_0)/(RTFB_1)$  calculated for different temperatures, we evaluated the monolayer capacities ( $\bar{N}_m$ ) according to eqn. 20. Table III summarizes the monolayer capacities for the adsorption systems investigated.

For the purpose of calculating the pre-exponential factor of Henry's constant,

TABLE II  
PARAMETERS CHARACTERIZING THE APPROXIMATION IN EQN. 3

| Adsorbate        | Temp. (°K) | $m$ | $s \cdot 10^6$ ( $l^2/g^2$ ) | $\exp(B_0) \cdot 10^3$ ( $l/g$ ) | $-B_1RT \exp(B_0)$ ( $l^2/mole \cdot g$ ) | $-\exp(B_0)/(RTFB_1) \cdot 10^5$ ( $mole/g$ ) |
|------------------|------------|-----|------------------------------|----------------------------------|---|---|
| Benzene          | 328        | 9   | 53.40                        | 174.16                           | 1427.50                                   | 2.125   |
|                  | 343        | 9   | 10.46                        | 87.36                            | 400.24                                    | 1.907   |
|                  | 358        | 10  | 0.43                         | 48.82                            | 109.95                                    | 1.746   |
|                  | 373        | 9   | 0.15                         | 23.34                            | 28.63                                     | 1.902   |
| <i>n</i> -Hexane | 328        | 9   | 0.350                        | 19.89                            | 13.54                                     | 2.920   |
|                  | 343        | 9   | 0.043                        | 11.59                            | 5.18                                      | 2.594   |
|                  | 358        | 9   | 0.014                        | 7.03                             | 1.51                                      | 3.266   |
|                  | 373        | 9   | 0.002                        | 4.48                             | 1.04                                      | 1.936   |
| Cyclohexane      | 328        | 6   | 0.113                        | 17.29                            | 9.98                                      | 2.996   |
|                  | 343        | 6   | 0.037                        | 10.28                            | 2.85                                      | 3.711   |
|                  | 358        | 6   | 0.043                        | 6.80                             | 1.81                                      | 2.552   |
|                  | 373        | 6   | 0.011                        | 4.35                             | 0.69                                      | 2.736   |

TABLE III

PARAMETERS CHARACTERIZING THE ADSORPTION OF BENZENE, *n*-HEXANE AND CYCLOHEXANE ON THE POROUS GLASS BEADS

| Adsorbate        | $\bar{N}_m \cdot 10^5$<br>(mole/g) | $\bar{\epsilon}$<br>(cal/mole) | $\bar{K} \cdot 10^{-4}$<br>(atm <sup>-1</sup> ) | $K_{mob} \cdot 10^{-4}$<br>at 358°K<br>(atm <sup>-1</sup> ) | $\bar{K}/K_{mob}$ | $\epsilon^* - \epsilon_{mob}$<br>(cal/mole) |
|------------------|------------------------------------|--------------------------------|---|---|-------------------|---|
| Benzene          | 1.920                              | 11200                          | 17.810  | 15.123  | 1.18              | 120   |
| <i>n</i> -Hexane | 2.679                              | 8600                           | 4.821   | 4.545   | 1.06              | 50  |
| Cyclohexane      | 3.00                               | 8000                           | 2.112   | 1.988   | 1.06              | 50  |

exp( $B_0$ ), we approximated the experimental  $B_0$  values by means of a first-degree polynomial according to eqn. 18 (see Fig. 6). From the slopes of the straight lines in Fig. 6, the average adsorption energies ( $\bar{\epsilon}$ ) were calculated.  $\bar{K}$  values were evaluated from the intercepts and are summarized in Table III.

The correlation between the adsorption energies and adsorption isotherms is interesting (Fig. 7). The adsorption energy of *n*-hexane on the porous glass beads investigated is about 600 cal/mole higher than that for cyclohexane. This difference indicates that the behaviour of cyclohexane and *n*-hexane on the surface of the investigated porous glass beads is very similar, which is in excellent agreement with Fig. 7,

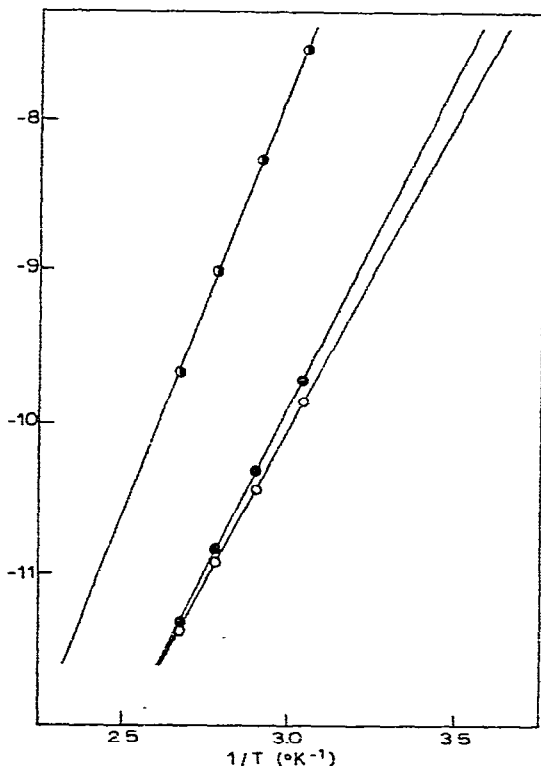
$$B_0 - \ln T$$


Fig. 6. Experimental functions ( $B_0 - \ln T$ ) versus  $1/T$ : ●, benzene; ●, *n*-hexane; ○, cyclohexane.

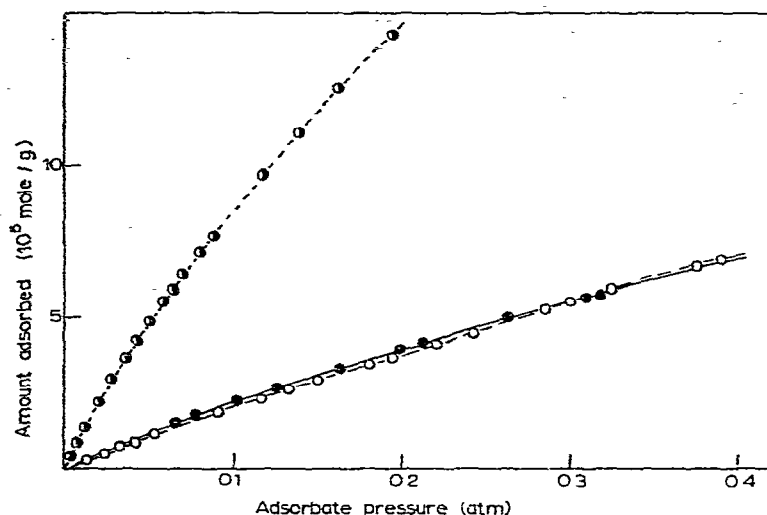


Fig. 7. Comparison of the adsorption isotherms of benzene (●), *n*-hexane (●) and cyclohexane (○) on the porous glass beads at 358°K.

where it can be seen that the adsorption isotherms are almost identical over the whole range of adsorbate pressures investigated.

For comparison, we also calculated  $K$  by assuming the mobile adsorption model (see eqn. 17). Then, the experimental points ( $B_0 - 0.5 \cdot \ln T$ ) were approximated by using a first-degree polynomial (eqn. 22 for  $r = 0.5$ ). Table III gives  $K$  values calculated for a temperature of 358°K, and also the ratio of the analogous constants  $\bar{K}$  and  $K_{\text{mob}}$ . It can be shown by using simple calculations that the shift of the energy distribution function on the energy axis caused by the difference between  $\bar{K}$  and  $K_{\text{mob}}$  is small. Let us denote the adsorption energy from eqn. 2 calculated for  $\bar{K}$  by  $\varepsilon^*$ , and the adsorption energy calculated for  $K_{\text{mob}}$  by  $\varepsilon_{\text{mob}}$ . Then, from eqn. 2, we obtain the relationship for calculating the shift of the energy distribution function:

$$\varepsilon^* - \varepsilon_{\text{mob}} = RT \ln (\bar{K}/K_{\text{mob}}) \quad (25)$$

The shifts of the distribution functions calculated according to eqn. 25 for the adsorption systems investigated are small in comparison with the observed adsorption energy (see Table III). It follows from Table III that the  $K$  values presented are dependent on the nature of the adsorbate, but they are not strongly affected by temperature at high temperatures. The values of  $\bar{K}$  are higher than the corresponding values evaluated for mobile adsorption. This result is in good agreement with the results of theoretical studies of the pre-exponential factor; it follows from these studies that  $K_{\text{loc}}$  is higher than  $K_{\text{mob}}$  (ref. 3).

Using the  $\bar{K}$  values in Table III, we calculated the energy distribution functions corresponding to eqn. 3<sup>9,10</sup>:

$$\chi(p(\varepsilon)) = \frac{-p^2}{F \ln 2 \cdot (RT)^2} \left[ \sum_{i=1}^m i B_i p^{i-1} \right] \cdot \exp \left( \sum_{i=0}^m B_i p^i \right) \quad (26)$$

In Fig. 8, the energy distribution functions (eqn. 26) for benzene on the porous glass beads investigated are plotted for the temperatures 328, 358 and 373 °K. These functions have two maxima, one being very distinct and the other much less distinct. With increasing temperature, the second maximum becomes smaller and thus a smaller heterogeneity of the adsorbent surface is observed.

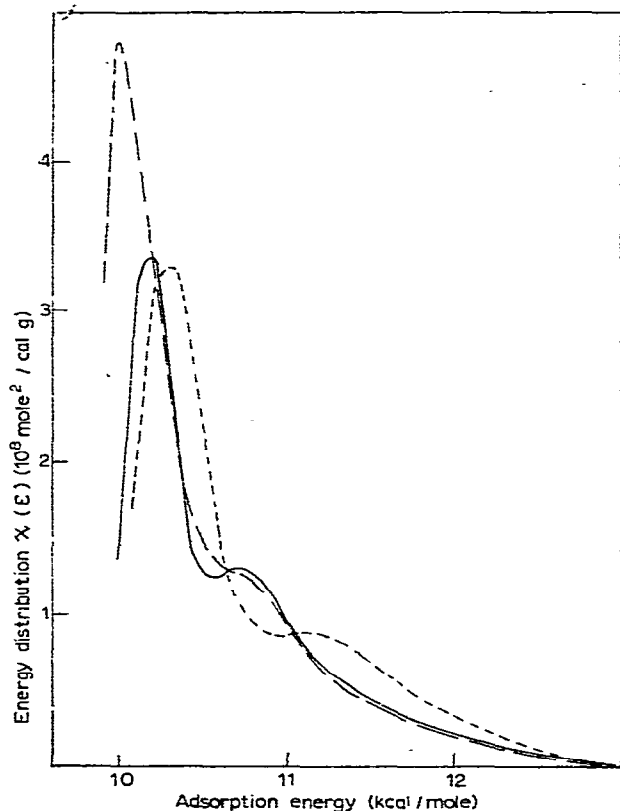


Fig. 8. Energy distribution functions for the benzene-porous glass beads adsorption system calculated according to eqn. 26 for different temperatures: 328°K (—); 358°K (— — —); 373°K (— · — · —).

The reason of this result is as follows. With increasing temperature, the probability of mobile adsorption increases. In contrast to the localized adsorption, in the mobile adsorption the molecules are not strictly connected with adsorption sites but can move freely on the surface. This effect consequently leads to more regular changes in adsorption energy differences, *i.e.*, smoothing of the shape of the distribution function.

In Fig. 9, the energy distributions of benzene, *n*-hexane and cyclohexane on the porous glass beads investigated, calculated for a temperature of 358 °K, and  $\bar{K}$  are compared. It follows that the most specific interactions with the surface of the adsorbent were shown by molecules of benzene. Two visible peaks in the energy distribution

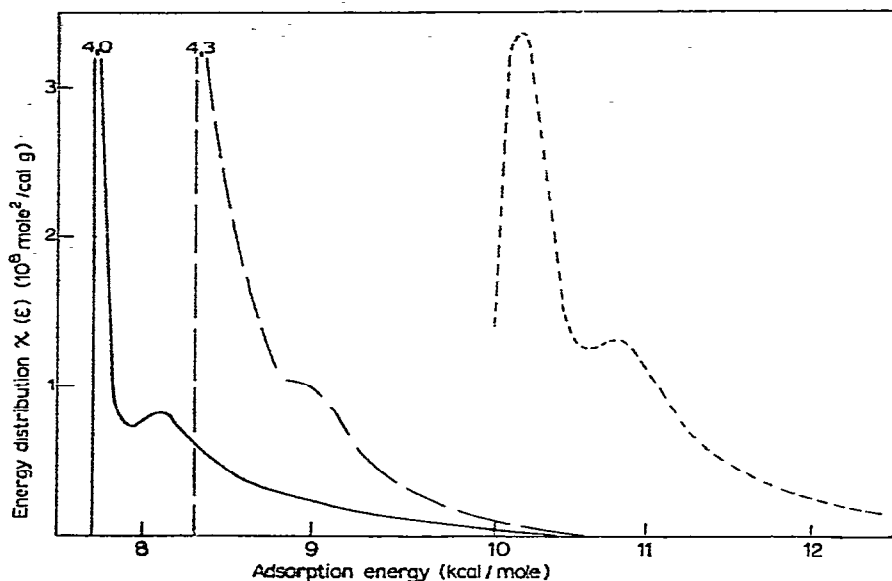


Fig. 9. Comparison of the energy distribution functions for benzene (—), *n*-hexane (---) and cyclohexane (— · —) on the porous glass beads at 358°K.

for benzene probably correspond to distinct types of hydroxyl groups that usually exist on silica or glass surfaces<sup>1,3</sup>. In contrast to the silica surfaces, the glass surfaces can also react with an adsorbing molecule by means of the boron atoms<sup>44</sup>.

The texture of the porous glass beads is homogeneous with respect to the pore size distribution (see Figs. 1 and 2). It follows from Figs. 1 and 2 that 95% of the total pore volume has pore radii between 100 and 200 Å. Hence we can say that this adsorbent does not have micropores, and the surface heterogeneity is connected rather with the chemical structure of the porous glass beads.

## REFERENCES

- 1 M. Jaroniec, W. Rudziński and S. Sokołowski, *Colloid Polym. Sci.*, 253 (1975) 164.
- 2 M. Jaroniec and W. Rudziński, *Colloid Polym. Sci.*, 253 (1975) 683.
- 3 M. Jaroniec, *Surface Sci.*, 50 (1975) 553.
- 4 W. Rudziński, A. Waksmundzki, R. Leboda, Z. Suprynowicz and M. Lasoń, *J. Chromatogr.*, 92 (1974) 25.
- 5 W. Rudziński, A. Waksmundzki, R. Leboda and M. Jaroniec, *Chromatographia*, 7 (1974) 663.
- 6 A. Waksmundzki, S. Sokołowski, M. Jaroniec and J. Rayss, *Vuoto*, 8 (1975) 113.
- 7 A. Waksmundzki, S. Sokołowski, J. Rayss, Z. Suprynowicz and M. Jaroniec, *Separ. Sci.*, 11 (1976) 29.
- 8 A. Waksmundzki, M. Jaroniec and Z. Suprynowicz, *J. Chromatogr.*, 110 (1975) 381.
- 9 Z. Suprynowicz, M. Jaroniec and J. Gawdzik, *Chromatographia*, 9 (1976) in press.
- 10 Z. Suprynowicz and M. Jaroniec, *J. Chromatogr.*, 117 (1976) 11.
- 11 A. Waksmundzki, M. Jaroniec and L. Łajtar, *Ann. Soc. Chim. Pol.*, 49 (1975) 1197.
- 12 M. Jaroniec, S. Sokołowski and G. F. Cerofolini, *Thin Solid Films*, 31 (1976) 321.
- 13 W. A. House and M. J. Jaycock, *J. Colloid Interface Sci.*, 47 (1974) 50.
- 14 W. Rudziński, M. Jaroniec, S. Sokołowski and G. F. Cerofolini, *Czech. J. Phys.*, 25B (1975) 891.
- 15 S. Sokołowski, M. Jaroniec and G. F. Cerofolini, *Surface Sci.*, 47 (1975) 429.

- 16 A. Clark, *The Theory of Adsorption and Catalysis*, Academic Press, New York, 1970, p. 24.
- 17 D. M. Young and A. D. Crowell, *Physical Adsorption of Gases*, Butterworths, London, 1962, pp. 114-116.
- 18 A. V. Kiselev and D. P. Poshkus, *Trans. Faraday Soc.*, 59 (1963) 1438.
- 19 N. N. Avgul, A. V. Kiselev and D. P. Poshkus, *Adsorption of Gases and Vapours on Homogeneous Surfaces*, Khimia, Moscow, 1975, p. 227.
- 20 D. H. Everett, *Surface Area Determination*, Butterworths, London, 1970, p. 181.
- 21 M. Jaroniec, *J. Colloid Interface Sci.*, 52 (1975) 41.
- 22 W. Rudziński, *Czech. J. Phys.*, 22B (1972) 432.
- 23 W. Rudziński, Z. Suprynowicz and J. Rayss, *J. Chromatogr.*, 66 (1972) 1.
- 24 A. Waksmundzki, W. Rudziński, Z. Suprynowicz and J. Rayss, *J. Chromatogr.*, 74 (1972) 3.
- 25 D. S. Jovanović, *Kolloid-Z. Z. Polym.*, 235 (1970) 1203.
- 26 M. Jaroniec, *Colloid Polym. Sci.*, 254 (1976) in press.
- 27 W. Rudziński and M. Jaroniec, *Surface Sci.*, 42 (1974) 552.
- 28 W. Rudziński and M. Jaroniec, *Ann. Soc. Chim. Pol.*, 49 (1975) 165.
- 29 S. E. Hoory and J. M. Prausnitz, *Surface Sci.*, 6 (1967) 377.
- 30 J. P. Hobson, *Can. J. Phys.*, 43 (1965) 1934.
- 31 W. Rudziński, A. Waksmundzki, Z. Suprynowicz and J. Rayss, *J. Chromatogr.*, 72 (1972) 221.
- 32 A. Waksmundzki, Z. Suprynowicz, J. Gawdzik and A. Dawidowicz, *Chem. Anal. (Warsaw)*, 19 (1974) 1033.
- 33 H. P. Hood and M. E. Nordberg, *U.S. Pat.*, 2,106,744 (1938).
- 34 W. Haller, *J. Chem. Phys.*, 42 (1965) 686.
- 35 W. P. Zdanov, *Dokl. Akad. Nauk SSSR*, 82 (1952) 281.
- 36 N. B. Volf, *Technical Glasses*, Pitman, London, 1961, Ch. X.
- 37 L. B. Nickols and J. M. Thorp, *Trans. Faraday Soc.*, 66 (1970) 1741.
- 38 L. Feitl, P. Lutovský, L. Sosnová and E. Smolková, *J. Chromatogr.*, 91 (1974) 321.
- 39 N. W. Akshinskaya, T. A. Baygubekova, A. V. Kiselev and V. C. Nikitin, *Kolloid Zh.*, 28 (1966) 164.
- 40 E. P. Barrett, L. G. Joyner and P. P. Halenda, *J. Amer. Chem. Soc.*, 73 (1951) 373.
- 41 A. Wheeler, in P. H. Emmet (Editor), *Catalysis*, Vol. II, Reinhold, New York, 1955, p. 105.
- 42 D. Dollimore, G. R. Heal and D. R. Martin, *J. Chromatogr.*, 50 (1970) 209.
- 43 J. F. K. Huber and R. G. Gerritse, *J. Chromatogr.*, 58 (1971) 137.
- 44 M. L. Hair and A. M. Filbert, *Res. Develop.*, 20 (1969) 34.